Electron Correlation

International Edition: DOI: 10.1002/anie.201501887
German Edition: DOI: 10.1002/ange.201501887

A Practicable Real-Space Measure and Visualization of Static Electron-Correlation Effects**

Stefan Grimme and Andreas Hansen*

In memory of Tom Ziegler

Abstract: *The inclusion of dynamical and static electron correlation (SEC) is mandatory for accurate quantum chemistry (QC). SEC is particularly difficult to calculate and hence a qualitative understanding is important to judge the applicability of approximate QC methods. Existing scalar SEC diagnostics, however, lack the important information where the SEC effects occur in a molecule. We introduce an analysis tool based on a fractional occupation number weighted electron density (ρ^{FOD}) that is plotted in 3D for a pre-defined contour surface value. The scalar field is obtained by finite-temperature DFT calculations with pre-defined electronic temperature (e.g. TPSS at 5000 K). FOD plots only show the contribution of the "hot" (strongly correlated) electrons. We discuss illustrative plots for a broad range of chemical systems from small molecules to large conjugated molecules with polyradicaloid character. Spatial integration yields a single number which can be used to globally quantify SEC.*

Quantum chemical methods for electronic structure require the inclusion of electron correlation (EC, also called "many-body") effects when aiming at quantitative accuracy. The EC is commonly divided into dynamical and static (non-dynamical, SEC) contributions.[1] Molecular systems with strong SEC are represented, for example, by covalent bond breaking, bi- or polyradicals, or certain classes of transition-metal complexes. They are usually characterized by small energy gaps between frontier orbitals and hence, appearance of many equally important determinants in electronic wave functions while systems dominated by dynamic EC exhibit a large HOMO–LUMO gap and are well described by a single Hartree–Fock (HF) or Kohn–Sham (KS) configuration. The accurate account of SEC is challenging in wave function theory (WFT) as well as density functional theory (DFT; see Refs. [2–4] for overviews). Beside the pure quantification of SEC to obtain reliable molecular energies or structures for such so-called multi-reference (MR, termed also multi-configurational) systems, its qualitative understanding is also important. Such insight is the key to estimating the accuracy or even applicability of approximate electronic structure methods and hence, many qualitative SEC measures have been developed (see Ref. [5] for an overview). Normally these metrics provide a single number for an entire molecule which misses the important information in which chemical part of the molecule SEC effects occur. If, for example, a C–C bond breaks in a long alkane chain, only the directly involved or spatially close-lying groups will be "strongly correlated" while most of the electrons are just "spectators" in this process and behave as in a large gap, closed-shell ("insulator") system. We think that the spatial distribution of SEC in molecules is important for the practical application and further development of approximate WFT and DFT methods. The incorrect treatment of SEC in contemporary Kohn–Sham (KS)-DFT approximations has been noted repeatedly[3,6] and is related to practically important topics, such as spin-state splitting or magnetic properties.[7]

Herein we introduce a simple, yet physically sound real-space measure of SEC based on fractional orbital occupation (FO), finite-temperature DFT (also called "Fermi-smearing"[8] technique). This well-established method has recently been re-discovered to solve the SEC problem for typical chemical model problems.[9,10] The fact that FO in standard KS-DFT calculations at several thousands of Kelvin electronic temperature recover important SEC effects was observed in our group in conjunction with the automated dynamics based calculation of electron impact mass spectra (QCEIMS method[11]). In that work, finite-temperature(FT)-DFT was merely used to facilitate self-consistent field (SCF) convergence, but it was already noted that dissociation energies improve up to some optimal electronic temperature in agreement with the observations in Ref. [9]. Herein we do not consider electronic energies but instead employ FT-DFT to derive a practicable routine tool to analyze SEC in any chemical system. We propose a real-space function ρ^{FOD} of position vector r termed fractional orbital density (FOD) given by [Eq. (1)]:

$$\rho^{\mathrm{FOD}}(r) = \sum_{i}^{N} (\delta_1 - \delta_2 f_i) |\varphi_i(r)|^2 \qquad (1)$$

where φ_i are molecular spin orbitals, f_i are the FO numbers ($0 \le f_i \le 1$) and the sum is taken over all electronic single-particle levels in the system. They are obtained by solving self-consistently the KS-SCF equations which minimize the free-

[*] Prof. Dr. S. Grimme, Dr. A. Hansen
Universität Bonn
Mulliken Center for Theoretical Chemistry
Beringstrasse 4, Bonn, 53115 (Germany)
E-mail: grimme@thch.uni-bonn.de

[**] This work was supported by the DFG in the framework of the SFB 813 ("Chemistry at Spin Centers"). We thank members of the Grimme group for helpful discussions as well as J. Mekelburger and Dr. U. Huniar (COSMOLogic) for technical support. The free of charge availableness of the ORCA and the UCSF Chimera software is gratefully acknowledged.

Supporting information for this article is available on the WWW under http://dx.doi.org/10.1002/anie.201501887.

electronic energy G_{el} [Eq. (2)]

$$G_{el} = E_{el} - T_{el}S_{el} \quad (2)$$

with SCF energy E_{el} and the electronic entropy [Eq. (3)]

$$S_{el} = k\sum_{i}^{N} f_i \ln f_i + (1-f_i)\ln(1-f_i) \quad (3)$$

at electronic temperature T_{el}. This process, and in particular the entropy,[12] accounts physically for SEC and the solution corresponds to an ensemble of excited states. FT-DFT is implemented in many quantum chemistry programs as well as periodic solid-state codes. In Equation (1) we chose the constants δ_1 and δ_2 to be unity if the level is lower than the Fermi energy E_F while they are zero and -1, respectively, for levels higher than E_F. By this definition only the fractionally occupied (i.e., f_i different from zero or one, respectively) levels sum up, or in other words, the so defined FOD yields for each point in real space only the contribution of 'hot' or strongly correlated electrons. An alternative weighting scheme for the orbital densities $|\varphi_i(r)|^2$ would use the factor $f_i \ln f_i + (1-f_i)\ln(1-f_i)$. The FOD which is loosely related to the Fukui function[13] can be obtained from any WFT or DFT electronic structure method that provides fractionally occupied orbitals. Analysis of scalar fields for understanding complex chemical properties has recently become popular, for example, in the NCIplot approach to visualize non-covalent interactions.[14]

Herein we propose to apply this procedure with standard density functionals, such as TPSS, B3LYP, PBE0, or M06-2X,[15] and plotting $\rho^{FOD}(r)$ for pre-defined contour surface values σ with graphics software (e.g. CHIMERA,[16] see Supporting Information for details). All calculations were performed with a development version of the ORCA program[17] (the FOD analysis will be part of its next release, for TURBOMOLE interfacing scripts see Ref. [18]). Unless noted otherwise, optimized TPSS-D3(BJ)[19]/def2-TZVP[20] geometries were used (see Supporting Information). Note that integration of the FOD over all space yields a single size-extensive number (termed N_{FOD}) which (similar to the magnitude of S_{el}) can be used to globally quantify SEC (see below). This value correlates well with other common SEC diagnostics[5,21] (see Supporting Information for a detailed analysis of small and medium-sized molecules).[22]

To ensure general applicability, one remaining problem has to be solved. The FO numbers (and N_{FOD} or TS_{el}) as determined from the Fermi–Dirac distribution [Eq. (4)]

$$f_i = \frac{1}{e^{(\varepsilon_i - E_F)/kT_{el}} + 1} \quad (4)$$

strongly depend on the difference of the orbital energy ε_i to the Fermi energy, that is, essentially the orbital energy gaps. Their values depend almost linearly on the amount of non-local Fock exchange admixture (termed a_x) in the chosen (hybrid) density functional. In our tested series of prototype functionals a_x amounts to 0% (TPSS), 20% (B3LYP), 25% (PBE0), and 54% (M06-2X). The dependence of the optimal electronic temperature on a_x has been noted in Refs. [9,11]. We have already proposed[11] to linearly increase T_{el} with a_x and use the established relation $T_{el} = 20000\ \mathrm{K} \times a_x + 5000\ \mathrm{K}$ herein. FT-DFT in this setting furthermore provides a reasonable energetic description of strongly correlated systems but this will be studied separately and we concentrate herein on the FOD and qualitative considerations. Figure 1 shows two representative examples, the notoriously difficult ozone molecule[23] and a stretched terminal C–C bond of an *n*-octane conformer as prototype for breaking a covalent bond. According to these plots, the shape of the contour surfaces is very similar for all tested functionals irrespective of the fact that the gap changes by several eV from TPSS to M06-2X. This is an important result that justifies the a_x-adjusted temperature approach and underlines the physical signifi-

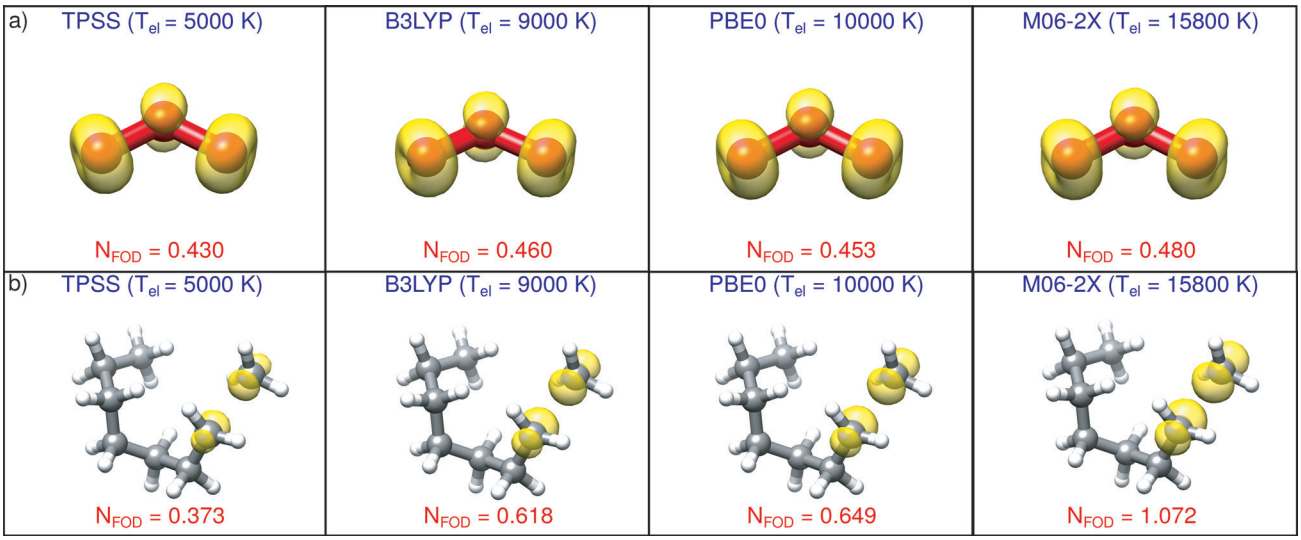

Figure 1. Dependence of FOD plots (def2-TZVP) on the electronic temperature (or functional) at $\sigma = 0.005\ e\,\mathrm{Bohr}^{-3}$ for a) ozone and b) *n*-octane with stretched terminal C–C bond (FOD in yellow).

cance of the FOD analysis. Note that significant FOD is delocalized in ozone, that is, the whole molecule is strongly correlated while in the octane example the FOD is concentrated to the breaking bond in accordance with chemical intuition.

Having shown that the FOD can be obtained consistently and efficiently, we analyze its meaning on more chemical grounds. For simplicity we use TPSS/def2-TZVP at 5000 K in the following and note that very similar plots are obtained with other functionals and basis sets (see Supporting Information). The FOD is identical for restricted and unrestricted (non-spin-symmetry broken) SCF treatments. It can be applied to arbitrary spin states as long as they are in principle accessible to KS-DFT.

The N_{FOD} values for large-gap insulators, such as alkanes, are very small ($<10^{-3}$) but increase as expected for systems with double bonds, such as benzene, to values of about 10^{-2}, and even to 0.2 for more strongly correlated polyenes, such as octatetraene. Nevertheless, we do not consider stable, unsaturated organic molecules as being strongly correlated which is in agreement with common global SEC measures. We estimated a lower limit for the default contour value σ such that for these systems nothing or only very small features are visible in an FOD plot. We have further investigated several molecules with an increasing degree of SEC (the anti-aromatic cyclobutadiene molecule in D_{2h} symmetry,[10,24] the CN radical,[25] and the transition state (TS) for insertion of Be into H_2)[26] to find σ values which yield reasonable shaped contour surfaces (see Supporting Information for further examples). After some testing we arrived at a final default value of $\sigma = 0.005$ e Bohr^{-3} which will be used in the following. It is important to note that this value should not be changed to allow comparison of different systems. In critical cases, however, we suggest to check also the FOD plot with a smaller value of $\sigma = 0.002$ (see Supporting Information). As a density, the FOD is strictly positive everywhere and in simple cases resembles orbital densities (e.g. of π-shape in larger acenes or polyenes)[27] while for an idealized "metal" with complete orbital degeneracy it is simply given by the total charge density. The FOD and corresponding N_{FOD} values for typical MR and non-MR cases are shown in Figure 2 and discussed below.

One frequently studied reaction suffering from MR effects is the insertion of a beryllium atom into the H_2 bond. While the reactants (separated by 4 Bohr, see Figure 2a) do not show significant SEC, the corresponding transition state (separated by 2.825 Bohr) is clearly identified by a large and delocalized FOD (and large N_{FOD} value) as a very difficult MR system (see Figure 2b) requiring elaborate MR methods.[26] The anti-aromatic cyclobutadiene in its minimum geometry (see Figure 2e) is also critical in terms of SEC and the developing biradicaloid character which is maximum for the D_{4h} symmetric transition state is clearly visible. The seemingly simple closed-shell molecule S_8^{2+} (Figure 2c) shows a surprisingly large FOD, particularly at the middle 1,5-positions. This explains the high sensitivity of the length of this (half-formed) bond on the choice of the DFT functional and the amount of a_x included.[19,28] The chemical importance of transition states with biradicaloid character is, for example, reflected in the long-standing controversy about "allowed" and "forbidden" cycloaddition reactions.[29] The FOD plots of the concerted ("DA cts") and the "gauche-in" ("DA nts", stepwise biradical mechanism) transition states of the Diels–Alder reaction of ethene with 1,3-butadiene (see Ref. [29] for details) are good examples for the predictive power of our analysis. The SEC of the biradicaloid transition state is clearly visible in contrast to the concerted case where nothing is found in the plot and N_{FOD} is one order of magnitude smaller. Another famous example for biradicaloid character is singlet (^1A_g) *p*-benzyne.[30,31] While the FOD plots (see Figure 2i–l) for *o*-benzyne, *m*-benzyne, and the first excited triplet state ($^3B_{1u}$) of *p*-benzyne show (almost) no density, the singlet *p*-benzyne has a large and delocalized FOD (and one order of magnitude larger N_{FOD}) which reflects its well-established MR character.[31] Comparing the FOD plots of anthracene (Figure 2q) and heptacene (Figure 2s), it is evident that the known increase of the polyradicaloid character of the non-bridging C atoms in linear polycyclic hydrocarbons with its number of fused rings and towards the middle of the molecule[32] is well reflected by the FOD analysis. Even more illustrative for such cases is the FOD plot for the recently published tetracyclopenta[def,jkl,pqr,vwx]tetraphenylene (TCPTP, Figure 2t).[33] The proposed anti-aromaticity and tetraradicaloid character of this molecule is clearly identified with the FOD analysis. FOD plots may also be very helpful in transition-metal chemistry. For example, the closed-shell 1,1′-dipentylferrocene complex (Figure 2p) correctly shows a small, rather localized FOD only at the iron center. Ferrocene is problematic with HF and MP2 but not with most density functionals including hybrids. With HF the C–M bonds are too long and not too short as often the case for bonds involving strong SEC. The too short bonds at the MP2 level were attributed to the neglect of single excitations[34] but not to the presence of SEC as corroborated by the FOD plot. In contrast, the electronically difficult transition state of the isomerization between the peroxo- and bis-(μ-oxo) form of the $[(Cu(C_2H_8N_2))_2O_2]^{2+}$ complex[35] has a large and delocalized FOD (Figure 2o). This is even more pronounced for the reactant complex[36] of the reaction of Ni^0 with NH_3 (Figure 2m). The same holds for the notoriously difficult permanganate anion (see Figure 2n), while the heavier Tc and Re homologous lack any significant FOD features in agreement with earlier theoretical results.[37] Further critical test cases are open-shell systems. The FOD of the cyanide radical (Figure 2d) is large and delocalized over the bond thus correctly identifying this molecule as difficult case for most QC methods.[25] However, radicals do not necessarily have a large FOD and the ones with relatively local SEC effects may not be problematic in standard WFT or DFT treatments. Often, these cases involve localized spin-centers on metal atoms or open-shell functional groups in organic molecules. Figure 2h,r show the persistent TEMPO[38] and trityl radicals, respectively. In agreement with chemical intuition, the FOD is spatially localized and relatively small. Hence, both radicals can be treated with single-reference methods although the trityl radical shows a large spin-contamination in unrestricted HF wave functions and is considered as a borderline case.[39] The slightly more delocal-

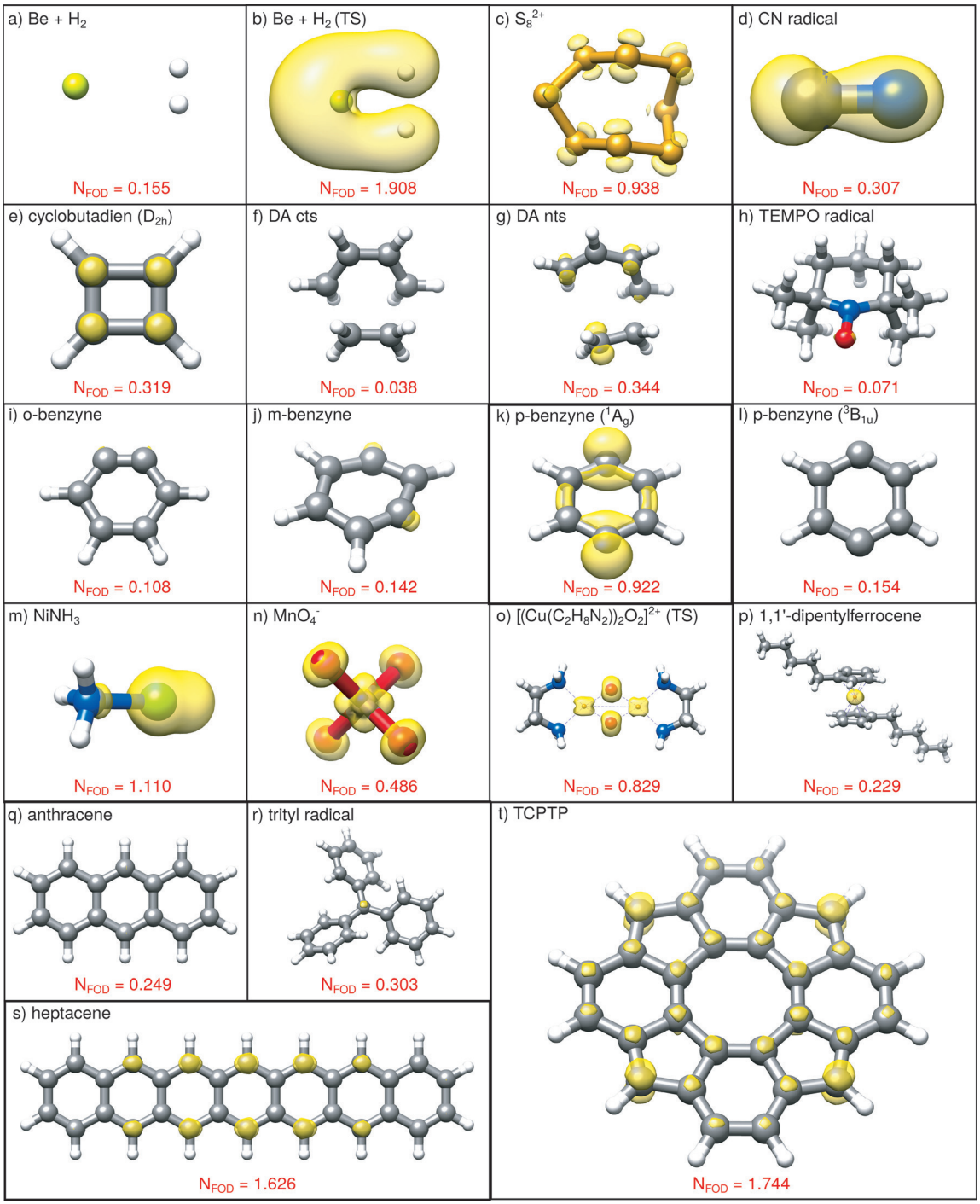

Figure 2. FOD plots at $\sigma = 0.005$ e Bohr^{-3} (TPSS/def2-TZVP (T = 5000 K) level) for various molecules (FOD in yellow).

ized FOD of the trityl radical becomes visible at a lower ($\sigma = 0.002$ e Bohr^{-3}) contour cut-off (see Supporting Information).

The last example is a 'real' application of biological importance, methylcobinamide and the related cobinamide radical cation. The plot of the cobinamide radical (Figure 3b) shows an about twice as large FOD compared to the closed-shell methylcobinamide (Figure 3a) but of still rather localized character. This situation is consistent with the conclusions from recent studies for this system[40] that GGA functionals (or hybrid functionals with $a_x < 0.15$) are safely applicable to describe the Co–C bond dissociation. Note that in this relatively large molecule, no spurious FOD appears which qualifies our method as a robust tool also for very extended systems. Since the FOD is relatively insensitive to the theoretical level employed, fast computations (less than 30 min computation time) using small basis sets can be conducted to analysis SEC for this example.

We have presented a routinely applicable analysis tool to improve the understanding of electronic correlation effects in molecules. It is based on a well-defined (observable-like)

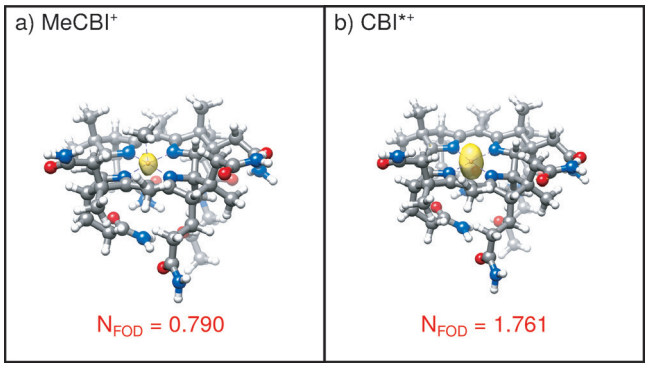

Figure 3. FOD plots at $\sigma = 0.005$ e Bohr^{-3} (TPSS/TZVP[41] ($T = 5000$ K) level) for a) methylcobinamide, and b) the cobinamide radical cation (FOD in yellow). The molecules correspond to reactant and product after the dissociation of a methyl radical.

fractional occupation number weighted electron density (FOD) that is plotted in 3D for a pre-defined contour surface value. The FOD can be consistently and efficiently obtained by finite-temperature DFT calculations with a variety of standard density functionals. Hence, the FOD analysis is a much faster and more illustrative tool to identify SEC in molecules (and for large systems almost without any alternative) than performing an elaborate coupled-cluster calculation and using common global measures as the T_1 diagnostics or the largest T_2 amplitudes. The information contained in these metrics is also contained in N_{FOD} (see Supporting Information) but in addition the FOD plot directly identifies the 'hot' and chemically active electrons in the molecule. Furthermore, the FO numbers may be used to select a proper active space for subsequent MR or CASSCF calculations (see Supporting Information for an illustrative example).

Our current empirical evidence is based on a (more or less) arbitrary chosen, limited number of typical test cases with supposedly absent or present SEC. According to the many tests, the approach seems to be very robust and we feel confident to draw the following general recommendations for choosing decent quantum chemical methods based on three categories: 1) If there is no visible FOD, the electronic structure is of single-reference nature and common (double) hybrid density functionals should provide very reasonable results. 2) If there is a significant yet relatively localized FOD visible, hybrid functionals with low Fock-exchange or even better, semi-local (non-hybrid) GGA functionals are preferred and HF or MP2 methods should be avoided. 3) A large and rather delocalized FOD indicates a true multi-reference (MR) case which should be treated by appropriate MR-WFT methods or for larger molecules with FT-DFT. We hope that these rules of thumb will help the community to conduct more reliable quantum chemistry in the future. Using the FOD for developing more accurate DFT methods is being investigated in our laboratory.

Keywords: density functional theory · Fermi-smearing · biradicals · multi-reference diagnostic · non-dynamical correlation

How to cite: *Angew. Chem. Int. Ed.* **2015**, *54*, 12308–12313
Angew. Chem. **2015**, *127*, 12483–12488

[1] a) T. Helgaker, P. Jørgensen, J. Olsen, *Molecular Electronic-Structure Theory*, Wiley, New York, **2000**; b) J. W. Hollett, P. M. W. Gill, *J. Chem. Phys.* **2011**, *134*, 114111.
[2] a) P. G. Szalay, T. Müller, G. Gidofalvi, H. Lischka, R. Shepard, *Chem. Rev.* **2012**, *112*, 108–181; b) D. I. Lyakh, M. Musial, V. F. Lotrich, R. J. Bartlett, *Chem. Rev.* **2012**, *112*, 182–243.
[3] A. J. Cohen, P. Mori-Sanchez, W. Yang, *Chem. Rev.* **2012**, *112*, 289–320.
[4] a) S. Grimme, M. Waletzke, *J. Chem. Phys.* **1999**, *111*, 5645; b) M. Filatov, *WIREs Comput. Mol. Sci.* **2015**, **5**, 146–147.
[5] U. R. Fogueri, S. Kozuch, A. Karton, J. M. L. Martin, *Theor. Chem. Acc.* **2013**, *132*, 1291–1230.
[6] a) G. I. Csonka, J. P. Perdew, A. Ruzsinszky, *J. Chem. Theory Comput.* **2010**, *6*, 3688–3703; b) A. D. Becke, *J. Chem. Phys.* **2014**, *140*, 18A301; c) J. Gräfenstein, D. Cremer, *Theo. Chem. Acc.* **2009**, *123*, 171–182; d) E. Kraisler, G. Makov, N. Argaman, I. Kelson, *Phys. Rev. A* **2009**, *80*, 032115.
[7] a) F. Neese, *Coord. Chem. Rev.* **2009**, *253*, 526–563; b) L. V. Slipchenko, A. I. Krylov, *J. Chem. Phys.* **2002**, *117*, 4694–4708.
[8] N. D. Mermin, *Phys. Rev.* **1965**, *137*, A1441.
[9] J.-D. Chai, *J. Chem. Phys.* **2012**, *136*, 154104.
[10] A. D. Becke, *Top. Curr. Chem.* **2014**, 1–12.
[11] S. Grimme, *Angew. Chem. Int. Ed.* **2013**, *52*, 6306–6312; *Angew. Chem.* **2013**, *125*, 6426–6433.
[12] P. Gersdorf, W. John, J. P. Perdew, P. Ziesche, *Int. J. Quantum Chem.* **1997**, *61*, 935–941.
[13] D. Peng, W. Yang, *J. Chem. Phys.* **2013**, *138*, 184108.
[14] E. R. Johnson, S. Keinan, P. Mori-Sanchez, J. Contreras-Garcia, A. J. Cohen, W. Yang, *J. Am. Chem. Soc.* **2010**, *132*, 6498–6506.
[15] a) J. Tao, J. P. Perdew, V. N. Staroverov, G. E. Scuseria, *Phys. Rev. Lett.* **2003**, *91*, 146401; b) A. D. Becke, *J. Chem. Phys.* **1993**, *98*, 5648–5652; c) P. J. Stephens, F. J. Devlin, C. F. Chabalowski, M. J. Frisch, *J. Phys. Chem.* **1994**, *98*, 11623–11627; d) J. P. Perdew, K. Burke, M. Ernzerhof, *Phys. Rev. Lett.* **1996**, *77*, 3865–3868; erratum J. P. Perdew, K. Burke, M. Ernzerhof, *Phys. Rev. Lett.* **1997**, *78*, 1396; e) C. Adamo, V. Barone, *J. Chem. Phys.* **1999**, *110*, 6158–6170; f) Y. Zhao, D. G. Truhlar, *Acc. Chem. Res.* **2008**, *41*, 157–167.
[16] E. F. Pettersen, T. D. Goddard, C. C. Huang, G. S. Couch, D. M. Greenblatt, E. C. Meng, T. E. Ferrin, *J. Comput. Chem.* **2004**, *25*, 1605–1612.
[17] a) F. Neese, *WIREs Comput. Mol. Sci.* **2012**, *2*, 73–78; b) F. Neese, ORCA—An Ab Initio, DFT and Semiempirical electronic structure package, Ver. 3.0—Current development version; Max Planck Institute for Chemical Energy Conversion: Mülheim a. d. Ruhr, Germany, **2015**.
[18] See http://www.thch.uni-bonn.de/.
[19] S. Grimme, S. Ehrlich, L. Goerigk, *J. Comput. Chem.* **2011**, *32*, 1456–1465.
[20] F. Weigend, R. Ahlrichs, *Phys. Chem. Chem. Phys.* **2005**, *7*, 3297–3305.
[21] M. K. Sprague, K. K. Irikura, *Theor. Chem. Acc.* **2014**, *133*, 1–12.
[22] A. Karton, I. Kaminker, J. M. Martin, *J. Phys. Chem. A* **2009**, *113*, 7610–7620.
[23] C. R. Nygaard, J. Olsen, *Mol. Phys.* **2013**, *111*, 1259–1270.
[24] H. Xu, S. Saebo, J. Pittman, U. Charles, *Struct. Chem.* **2014**, *25*, 635–648.
[25] P. M. Gill, J. A. Pople, L. Radom, R. H. Nobes, *J. Chem. Phys.* **1988**, *89*, 7307–7314.
[26] F. A. Evangelista, J. Gauss, *J. Chem. Phys.* **2011**, *134*, 114102.
[27] N. C. Craig, J. Demaison, P. Groner, H. D. Rudolph, N. Vogt, *J. Phys. Chem. A* **2015**, *119*, 195–204.

[28] T. Cameron, R. Deeth, I. Dionne, H. Du, H. Jenkins, I. Krossing, J. Passmore, H. Roobottom, *Inorg. Chem.* **2000**, *39*, 5614 – 5631.
[29] H. Lischka, E. Ventura, M. Dallos, *ChemPhysChem* **2004**, *5*, 1365 – 1371.
[30] W. Sander, *Acc. Chem. Res.* **1999**, *32*, 669 – 676.
[31] T. D. Crawford, E. Kraka, J. F. Stanton, D. Cremer, *J. Chem. Phys.* **2001**, *114*, 10638 – 10650.
[32] F. Plasser, H. PaŠalić, M. H. Gerzabek, F. Libisch, R. Reiter, J. Burgdörfer, T. Müller, R. Shepard, H. Lischka, *Angew. Chem. Int. Ed.* **2013**, *52*, 2581 – 2584; *Angew. Chem.* **2013**, *125*, 2641 – 2644.
[33] S. Nobusue, H. Miyoshi, A. Shimizu, I. Hisaki, K. Fukuda, M. Nakano, Y. Tobe, *Angew. Chem. Int. Ed.* **2015**, *54*, 2090 – 2094; *Angew. Chem.* **2015**, *127*, 2118 – 2122.
[34] C. Park, J. Almloef, *J. Chem. Phys.* **1991**, *95*, 1829 – 1833.
[35] D. G. Liakos, F. Neese, *J. Chem. Theory Comput.* **2011**, *7*, 1511 – 1523.
[36] M. Steinmetz, S. Grimme, *ChemistryOpen* **2013**, *2*, 115 – 124.
[37] R. M. Dickson, T. Ziegler, *Int. J. Quantum Chem.* **1996**, *58*, 681 – 687.
[38] D. Kubala, K. Regeta, R. Janeckova, J. Fedor, S. Grimme, A. Hansen, P. Nesvadba, M. Allan, *Mol. Phys.* **2013**, *111*, 2033 – 2040.
[39] A. Hansen, D. G. Liakos, F. Neese, *J. Chem. Phys.* **2011**, *135*, 214102.
[40] a) P. M. Kozlowski, M. Kumar, P. Piecuch, W. Li, N. P. Bauman, J. A. Hansen, P. Lodowski, M. Jaworska, *J. Chem. Theory Comput.* **2012**, *8*, 1870 – 1894; b) K. P. Kepp, *J. Phys. Chem. A* **2014**, *118*, 7104 – 7117; c) Z. Qu, A. Hansen, S. Grimme, *J. Chem. Theory Comput.* **2015**, *11*, 1037 – 1045.
[41] A. Schäfer, C. Huber, R. Ahlrichs, *J. Chem. Phys.* **1994**, *100*, 5829 – 5835.

Received: February 27, 2015
Published online: April 16, 2015

